Journal of Molecular Liquids 398 (2024) 124187

Contents lists available at ScienceDirect

Journal of Molecular Liquids

journal homepage: www.elsevier.com/locate/molliq

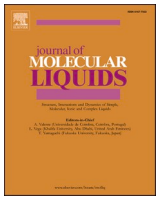

Liquid crystal-induced tunable circular dichroism in CdSe and ZnSe nanoplatelets

Urice N. Tohgha [a,b,*], Kyung Min Lee [a,b], Joseph M. Slocik [a], Ecklin M. Crenshaw [a,b], Zachary Marsh [a,b], Oscar A. Ovando [c], Alexander O. Govorov [c], Nicholas P. Godman [a,*]

[a] Materials and Manufacturing Directorate, Air Force Research Laboratory, Wright-Patterson Air Force Base, OH 45433, United States
[b] Azimuth Corporation, Beavercreek, OH 45324, United States
[c] Department of Physics and Astronomy, Ohio University, Athens, OH, United States

ARTICLE INFO

Keywords:
Chirality
Nanoplatelets
Liquid crystal
Circular dichroism
Composites
Films

ABSTRACT

Induced circular dichroism in CdSe and ZnSe nanoplatelets (NPLs) was demonstrated using chiral thermotropic liquid crystals (LCs). Firstly, NPLs were easily dispersed in cholesteryl oleyl carbonate (COC) LC via a simple intercalation chemistry-based approach. Extensive circular dichroism (CD) studies showed remarkably strong and reversible chiroptical properties for these composites as a function of temperature. NPL-COC composites displayed strong exciton-induced CD as well as high anisotropy g-factor values (in the case of CdSe NPLs). Secondly, induced chirality in CdSe NPLs was also demonstrated using right-handed (RH) and left-handed (LH) blue phase LCs. LC-induced chirality in nanoparticles was corroborated by theoretical studies which revealed coupling between the chiral molecular excitons and nonchiral nanocrystals. The temperature-tunability is a useful tool to switch the chirality on/off. This study presents an alternative approach to realize exciton-induced tunable circular dichroism in nanomaterials.

1. Introduction

Optical activity in semiconductor nanomaterials has attracted much interest in recent years [1–4] as a means of realizing chiral materials with chiroptical properties spanning the ultraviolet to visible region of the electromagnetic spectrum. The development of nanoparticles with chiroptical activity has been explored by direct synthesis in the presence of chiral molecules [2], post-synthetic ligand exchange with chiral molecules [3,5], and supramolecular assembly using chiral templates [6,7]. An alternative, and often underutilized, avenue for achieving chiral nanoparticle (NP) assembly is by utilizing the phase transition properties of liquid crystals (LCs) [8–11]. The incorporation of NPs into LC media has the potential of modifying the intrinsic optical properties of both systems resulting in tunable multifunctional LC composites [12–14]. However, reports on the benefits of incorporating nanomaterials into LC systems show inconsistencies due to the incompatibility of the pristine NPs and the LC media. The covalent attachment of mesogenic ligands to inorganic NPs has been shown to improve the dispersion of NPs in LCs [14–17], but such molecules are typically not commercially available and require custom synthesis [17,18]. More importantly, most of the aforementioned literature studies have mainly focused on plasmonic nanoparticles [18–20]. To the best of our knowledge, there are very few papers that show exciton-induced circular dichroism in semiconductor nanoparticles using liquid crystals [17,21].

The research reported herein is aimed at utilizing the phase transition of chiral LCs to drive NP assembly and impart unique chiroptical properties in CdSe and ZnSe nanoplatelets (NPLs). These were chosen because of the tendency of nanoplatelets to self-assemble as well as the potential morphological compatibility with LCs [22]. The LC (Cholesteryl oleyl carbonate) system used in this study have chiral properties at ambient temperatures which is appealing for potential practical applications. Cholesteryl oleyl carbonate (COC) liquid crystal is cheap, environmentally friendly and readily available unlike gelators that need to be synthesized [6]. In addition, other platforms such as cellulose nanocrystals require laborious preparation steps using concentrated acids [23].

Firstly, custom-synthesized CdSe and ZnSe NPLs capped with

* Corresponding authors at: Materials and Manufacturing Directorate, Air Force Research Laboratory, Wright-Patterson Air Force Base, OH 45433, United States (U.N. Tohgha).
E-mail addresses: urice.tohgha.ctr@us.af.mil (U.N. Tohgha), nicholas.godman.2@us.af.mil (N.P. Godman).

https://doi.org/10.1016/j.molliq.2024.124187
Received 14 July 2023; Received in revised form 17 January 2024; Accepted 31 January 2024
Available online 6 February 2024
0167-7322/Published by Elsevier B.V.

commonly used surface ligands (oleic acid and oleylamine) were dispersed COC. The resulting nanoplatelet-COC (NPL-COC) composites display unique and reversible chiroptical properties as a function of temperature. This work represents the first demostration of LC-induced circular dichroism in NPLs and is based on simple intercalation chemistry without the need for mesogenic nanoparticle ligands. The dispersion of NPLs in COC showed no siginificant change in the absorption features unlike literature studies on chiral thiol NPLs [24].

Secondly, the concept of LC-based chiral nanomaterials was demosntrated using blue phase LC mixtures (BPLCs) and NPLs. Liquid crytsal-driven assembly of CdSe NPLs was observed by using both left handed (LH) and right handed (RH) BPLCs. More, importantly, stable and chiral thin films (50 μm) of such composites were succesfully made. Extensive circular dichroism (CD) studies were done to explicitly study the optical activity of these composites.

2. Nanoparticles and COC characterization

The schematic representation of NPLs assembled within the helical structure of the cholesteric LC is presented in Fig. 1. Representative TEM images of NPL-LC are also shown. CdSe NPLs [24] were synthesized according to modified literature methods. The CdSe NPLs (1.4 nm thickness corresponding to 4.5 monolayers) [24] were specifically chosen as these materials were previously used to prepare chiral NPLs [24] with chiral thiols (cysteine). ZnSe NPLs (1.39 nm thick corresponding to 8 monolayers) [25] were synthesized according to literature methods [25]. Chiral ZnSe NPLs are less explored [26] and were chosen to demonstrate the versatility of the approach presented in this work. Nanoplatelets have large absorption cross section [27] compared to other nanomaterials, which makes them ideal for studying chiral nanomaterials with potentially high polarization discrimination ratios.

Details of NPL synthesis, characterization, and preparation of NPL-LC composites are reported in the experimental section. Fig. S1 shows the absorption spectra of pristine NPLs in hexane.

Initial characterization of the pristine LC was carried out prior to incorporating nanoparticles. Being a thermotropic LC, the chiral properties of COC occur at a specific temperature range (25–33 °C) which will be used to explore induced chirality in NPLs. The Differential Scanning Calorimetry (DSC) curve of COC (Fig. S2) has two phase transition temperatures: [28] smectic to cholesteric (20.2 °C) and cholesteric to isotropic (34 °C). Fig. S2 also shows temperature-dependent CD spectra of pure COC which was performed over a defined temperature range (30–40 °C). COC is a left handed (LH) cholesteric LC and selectively reflects LH circularly polarized light (CPL) as shown in Fig. S3 (a). The temperature-dependent behavior of the LC reflection is shown in Fig. S3 (b). To reduce the contribution of the COC reflection the temperature-dependent chiral properties of NPLs were studied at cholesteric temperatures (30–33 °C). CD measurements of NPL-COC composites were done in 1 mm cuvette (see ESI).

3. Results and discussion

3.1. CdSe NPLs in COC

Detailed exploration of CdSe NPL-COC was first carried out. CdSe NPL content in COC used in this study was set at 2 % and confirmed by thermogravimetric (TGA) studies as shown in Fig. S4. DSC characterization indicated that the LC helix is not compromised by the incorporation of CdSe NPLs as minimal shifts (2 °C) in the phase transition temperatures of composites compared to pure COC (Fig. S5) were observed.

The absorption and corresponding CD spectra for CdSe NPL-COC composites are shown in Fig. 2 (a) and (b) respectively. No chiroptical response is observed when the composite is heated to the isotropic temperature (40 °C) because the LC is not self-assembled into a helix. In the cholesteric phase, defined CD peaks become apparent as the NPLs self-assemble within the helical LC. CD spectra between 32 °C and 33 °C show the gradual decrease in CD peak intensity as the temperature is

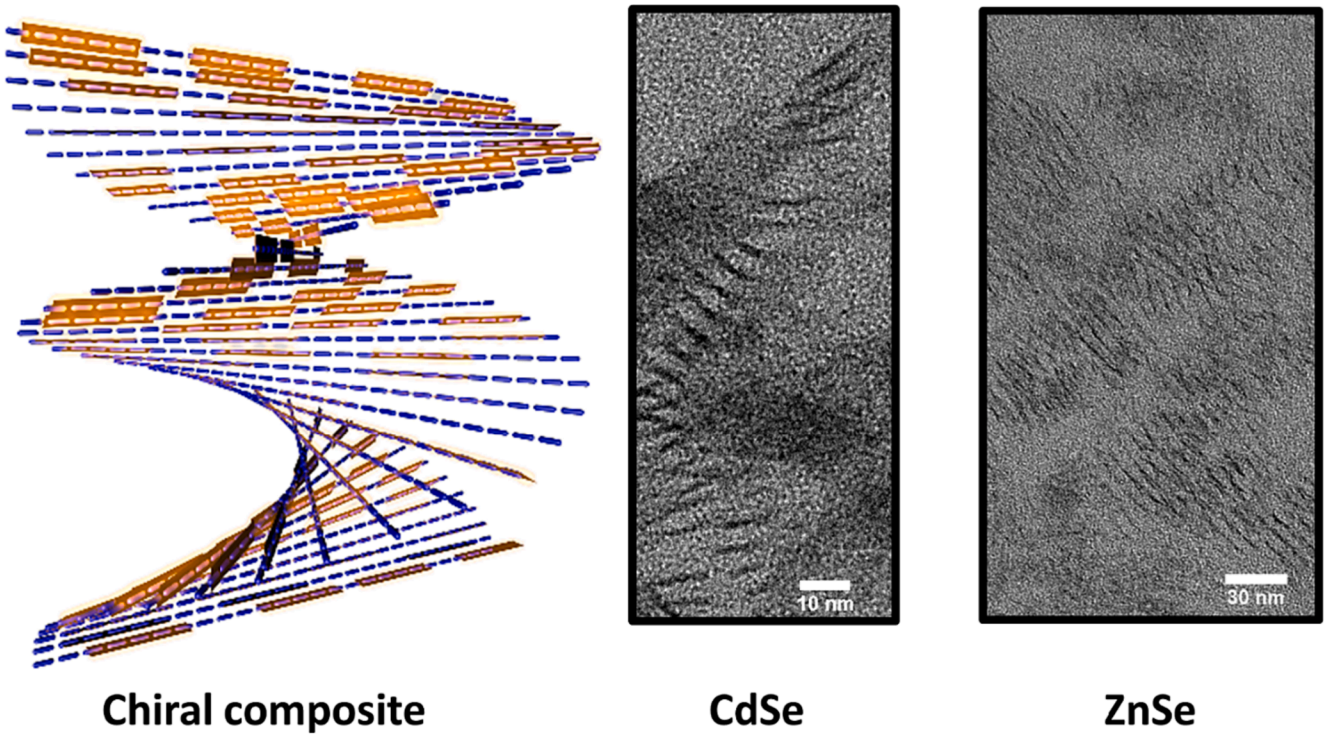

Fig. 1. NPLs (orange platelets) dispersed in chiral LC (left). TEM images of CdSe and ZnSe NPL-LC composites (right). Assembled NPLs can be seen in the TEM images. TEM of ZnSe NPLs show multiple 'stacks' of assembled NPLs. (For interpretation of the references to colour in this figure legend, the reader is referred to the web version of this article.)

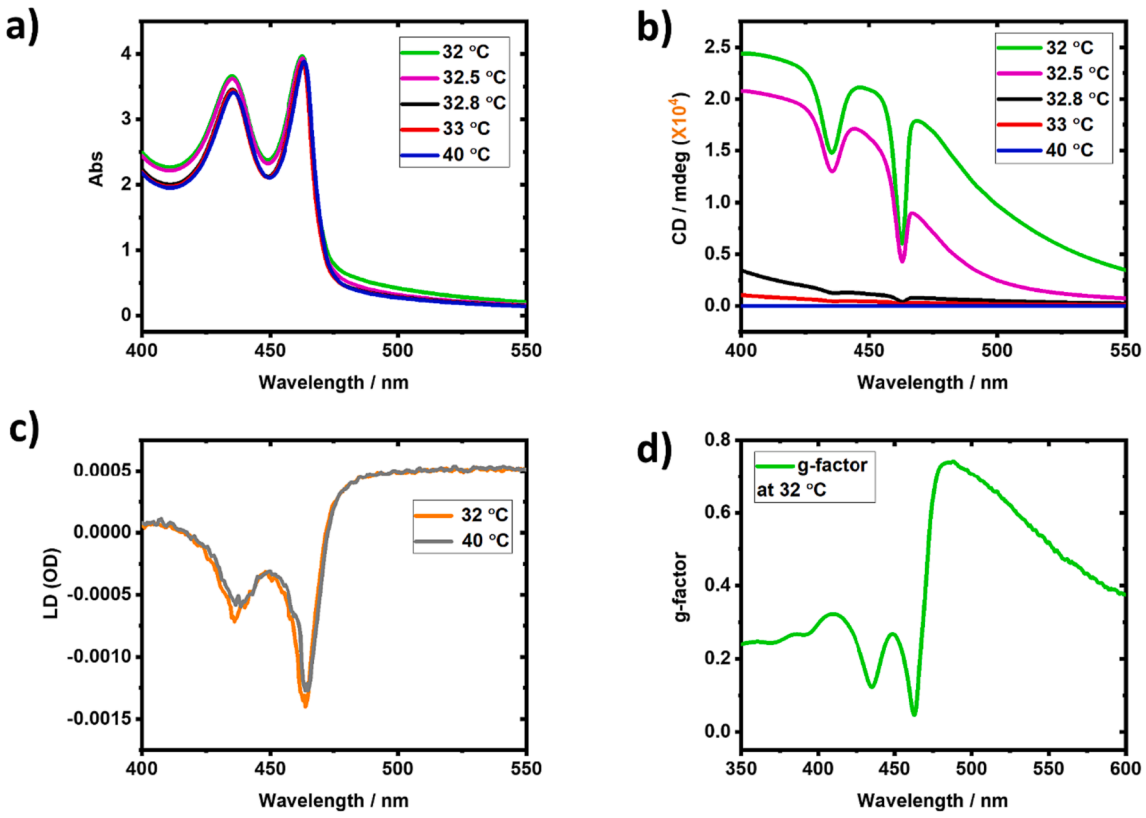

Fig. 2. Temperature independent absorption (**a**) and corresponding temperature-dependent CD (**b**) spectra of CdSe NPL-COC. Linear dichroism (LD) of CdSe NPL-COC (**c**). Anisotropy g-factor of CdSe NPL-COC at 32 °C (**d**). Composites with 2 % NPL content are shown.

increased. Interestingly, strong exciton induced CD peaks are observed at 434 nm and 462 nm without any wavelength shifts (compared to pristine NPLs). This is contrary to the cysteine stabilized zincblende NPLs from Gao et al. [24] where the authors observed a 29 nm red shift attributed to a change in solvent. The authors also reported significant peak broadening which is not observed in the COC composites. The NPL-LC composite approach eliminates the need for surface ligand exchange on the nanoparticle as well as the presence of solvents. More importantly, the ambiguity from the exact bonding and conformation of chiral thiols such as cysteine on nanoparticles is eliminated. The platelet morphology of NPLs may also play a role NPL-NPL coupling due to the tendency for NPLs to self-assemble [29]. It is worth noting that the chiroptical response is completely reversible (see Fig. 3). Fig. 2 (c) shows linear dichroism measurements at both cholesteric (32 °C) and isotropic (40 °C) temperatures. The matching LD spectra and extremely small signal suggests that LD effects do not significantly contribute to the

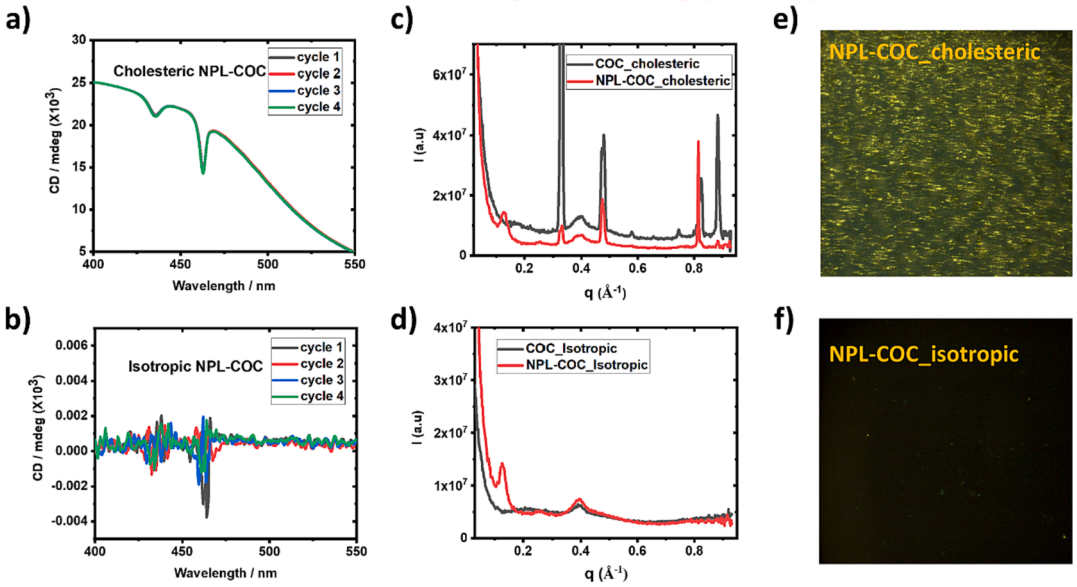

Fig. 3. CD thermal cycling studies (**a**, cholesteric and **b**, isotropic). Medium Angle X-ray scattering of NPL-COC and pure COC (**c**, cholesteric and **d**, isotropic). Polarized optical microscope (POM) images of NPL-COC under crossed polarizers (**e**, cholesteric and **f**, isotropic).

chiroptical properties of such nanocomposites. The CD spectra at 32 °C and 33 °C for pure COC (Fig. S2) are similar while the NPL-COC composites show more than an order of magnitude difference in CD intensity at the same temperatures. This was further confirmed by taking CD spectra of a representative sample at temperatures (30 °C and 31 °C) where the COC reflection is significantly minimized (Fig. S2). The CD spectra in Fig. S6 show the most intense NPL CD peaks at 30 °C which suggests that assembled nanoparticles (corroborated by TEM studies) significantly contribute to the chiroptical properties. These results suggest that the contribution of COC peaks to the NPL-COC CD spectra seem to be moderate. Anisotropy g-factor (ratio between molar CD and molar extinction coefficient) [30,31] calculations of NPL-COC were also performed. These calculations are based on the CD spectrum and corresponding absorption spectrum [30,31]. Fig. 2 (d) shows g-factor values of 0.12 (434 nm) and 0.06 (462 nm). These values are orders of magnitude higher than comparable g-factor values of thiol capped CdSe NPLs (Fig. S7).

Theoretical studies by Chen et al showed that absorption played a major role compared to reflection in the composite CD of helically stacked chromophores in cholesteric LC fluids [32]. This is consistent with the helical assembly of dye molecules in the cholesteric phases reported by Voss and coworkers [33]. We believe that a similar phenomenon is observed in the NPL-COC composites, where NPL-NPL coupling from the helically ordered NPs exhibit strong CD bands in the absorption region. Prasad and coworkers [34] studied QDs in a helical polymer and attributed the chiroptical properties to resonant coupling between QDs and the polymer. The temperature-dependent chiroptical properties of NPL-LC composites in our work suggests that resonant coupling likely occurs only in the cholesteric phase. In fact, the CD intensity is temperature-dependent as demonstrated by the results in Fig. 2 (b).

3.1.1. Effect of CdSe NPLs concentration in COC

The effect of CdSe NPL concentration was studied using composites containing 0.5 % NPL content (Fig. S8). While the lower NPL content still induces a chiroptical response, there is a more dominant LC reflection in the NPL-COC composites. As such, very weak CD peaks corresponding to the NPL were observed. NPL content is therefore critical to the LC induced CD profile and intensity. To better understand the effect of NPL content, LC composites with increased NPL loading were studied. NPL-COC composites with 3 % NPL showed significant aggregation which was corroborated by DSC. Fig. S9 shows peak shifts of 4° C to low temperatures accompanied by peak broadening. The increased NPL concentration can influence phase behavior of the LCs and 'compromise' the LC helix. Such NPL composites with significant aggregation are less likely to have reproducible chiroptical responses and were not extensively studied.

3.1.2. Thermal cycling, XRD and POM characterization of CdSe NPLs in COC LC

To further demonstrate the robust chiroptical properties from CdSe NPL-COC, thermal cycling CD measurements (4 cycles) were done at both cholesteric and isotropic temperatures. Fig. 3 (a) shows the retention of the CD peaks at cholesteric temperatures during 4 heating cycles while Fig. 3 (b) shows no CD peaks corresponding to the NPL at isotropic temperatures. Medium Angle X-ray Scattering (MAXS) was also utilized to study the effect of incorporating NPLs on the COC crystal structure as shown in Fig. 3 (c) (cholesteric) and (d) (isotropic). Interestingly, the most prominent COC peak (at about 0.35 $Å^{-1}$, Fig. 3 (c) is significantly attenuated by incorporating NPLs. This is attributed to NPL intercalation with the COC molecules. Two other peaks at 0.47 $Å^{-1}$ and 0.81 $Å^{-1}$ are maintained in NPL-COC which is attributed to the preservation of the COC helical structure. No COC peaks are observed at the isotropic phase (Fig. 3 (d)) as expected. More importantly, the MAXS results show that the nanoparticle peaks (at 0.13 $Å^{-1}$) are identical in both isotropic and cholesteric phases which supports the absorption spectra observed during the CD measurements.

Finally, polarized optical microscope (POM) images of NPL-COC composites were taken in the cholesteric (Fig. 3 (e)) and isotropic phases (Fig. 3 (f)) under crossed polarizers. The chiral NPL-COC composites can be observed in the cholesteric phase (bright greenish-yellow spots are NPLs) but not in the isotropic phase.

3.2. ZnSe nanoplatelets in COC LC

The concept of liquid crystal-driven circular dichroism in nanoparticles was also demonstrated using ZnSe NPLs which are considerably larger than CdSe NPLs as shown by the TEM images in Fig. S10. The difference in NPL dimensions is reflected in the preparation of ZnSe-COC composites. The preparation of 2 % ZnSe NPL content in COC led to significant aggregation and 'suppression' of the NPL peaks (Fig. S11). To avoid aggregation, ZnSe NPL-COC composites with 1 % NPL content were used for the study. DSC studies showed that 1 % ZnSe NPL in COC did not change the phase transition temperature of COC (Fig. S12). Fig. 4 (a) and (b) show temperature independent absorption and temperature-dependent CD spectra of ZnSe NPL-COC composites respectively. As was observed with CdSe NPLs, exciton induced CD peaks are observed at 325 nm and 347 nm without observed wavelength shifts compared to pristine ZnSe NPLs. A gradual decrease in CD peak intensity is observed as the temperature is increased from 29 °C to 40 °C. The chiroptical properties are attributed to LC-induced assembly of ZnSe NPLs as corroborated by the TEM image in Fig. S13. The anisotropy g-factor results in Fig. 4 (c) shows values of 0.001 at both 329 nm and 347 nm. The g-values are significantly less than those of the CdSe NPLs. Lu and coworkers recently showed a decrease in CD anisotropy factor in perovskite NPLs with higher number of monolayers [35]. The CdSe and ZnSe NPLs used in our study have 4.5 and 8 monolayers respectively, according to the literature papers used for the synthesis. However, the average thickness of both NPLs is identical. The reduced ZnSe NPL content in COC (1 %) compared to CdSe (2 %) may influence the chiroptical properties as well. Fig. 4 (d) shows identical spectra for the LD studies in both the cholesteric and isotropic phases. The results suggest that LD does not contribute in any significant way to the chiroptical properties of such nanocomposites. Polarized optical microscopy images of ZnSe-COC composites are shown at the cholesteric and isotropic phases in Fig. 4 (e) and (f) respectively.

ZnSe-COC composites comprised of a lower concentration of NPLs (0.5 %) were also used to explore the effect of concentration. Fig. S14 shows the absorption spectra and corresponding CD spectra at cholesteric and isotropic temperatures. The results are similar to the observations made with CdSe NPL-COC composites. The lower ZnSe NPL content leads to a chiroptical response but a more dominant LC reflection is observed due to the lower NPL content in the composites. As such, very weak CD peaks corresponding to the ZnSe NPLs were observed.

3.3. Theoretical investigation of NPL-COC composites

Theoretical understanding of NPL-COC composites was also pursued. We hypothesize, like Govorov and coworkers,[36,37] that the CD signal originates from the coupling of the chiral medium and the electronic excitations in the nanocrystals. The chiroptical data can be described in the following way: according to the general theory of the Cotton effect in molecules and nanocrystals,[38,39] a chiral absorption spectrum of a chiral system near an isolated resonance is formed of two slightly shifted terms:

$$\varepsilon_{res}(\omega) = \frac{\varepsilon_{res,0}(\omega + \Delta\omega_C/2) + \varepsilon_{res,0}(\omega - \Delta\omega_C/2)}{2},$$

where $\Delta\omega_C$ is the Cotton splitting indicating the formation of two chiral states in the system.$\Delta\omega_C$ is assumed to be small and can be either positive or negative. Correspondingly, the CD signal should be then written

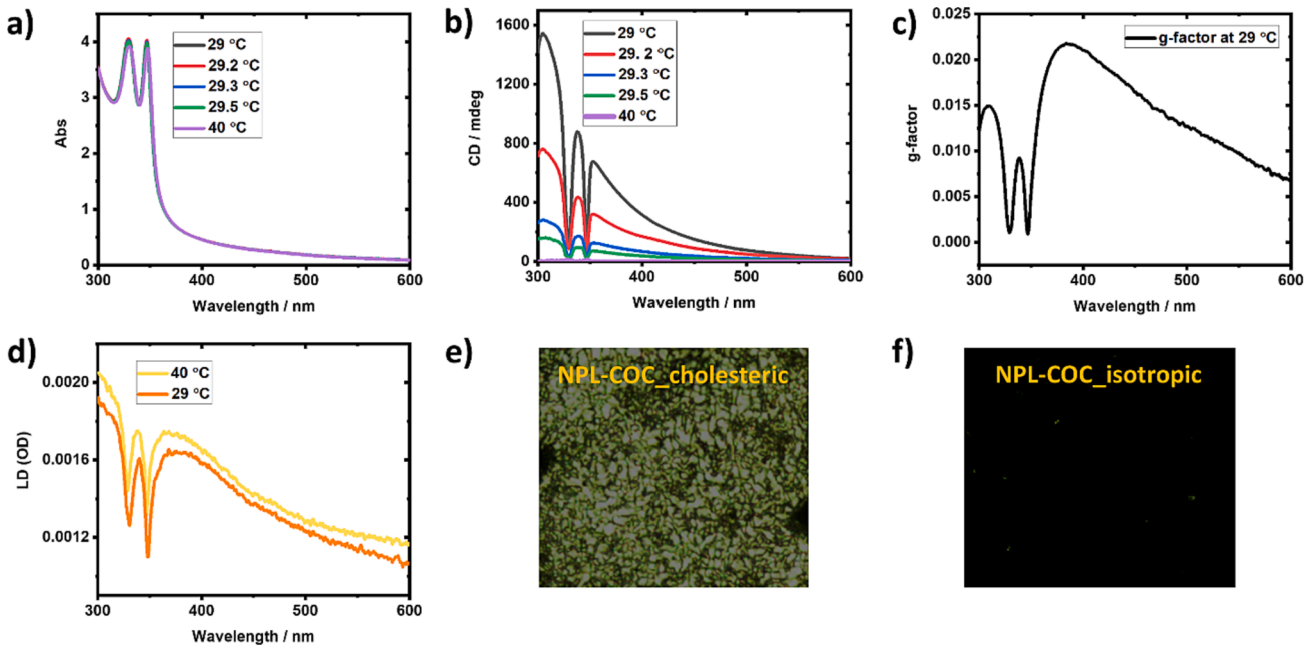

Fig. 4. Temperature independent absorption (**a**) and corresponding temperature-dependent CD (**b**) spectra of ZnSe NPL-COC. Anisotropy g-factor of ZnSe NPL-COC at 29 °C (**c**). LD of ZnSe NPL-COC (**d**). POM images in the cholesteric (e) and isotropic (f) phases are also shown. Composites with 1 % ZnSe NPL content are shown.

as

$$CD_{res} = \frac{\varepsilon_{res,0}(\omega + \Delta\omega_C/2) - \varepsilon_{res,0}(\omega - \Delta\omega_C/2)}{2} \approx \Delta\omega_C \frac{d\varepsilon_{res,0}}{d\omega}$$
$$= -\Delta\omega_C \cdot \frac{\lambda^2}{2\pi c} \frac{d\varepsilon_{res,0}}{d\lambda} \sim -\frac{d\varepsilon_{res,0}}{d\lambda} \quad (2)$$

Here, we should note that a similar processing of the CD signals was also proposed and utilized in the case of QDs with chiral ligands [4]. The CD spectra of the bio-conjugated QDs were fitted well with the bi-signate functions of the form $\frac{d\varepsilon_{res,0}}{d\lambda}$. However, for the NPLs studied here, the chiral-transfer effects (i.e., transfer of chirality from the LC matrix to NPLs) are expected to be much stronger than those in QDs [4] since the NPLs are much more optically active and absorbing. Indeed, in contrast to the work from Gil Markovich and coworkers,[4] the molecular medium-exciton interaction in our system is found to be strong, as high as 0.8 for the CdSe-COC system at $T < T_c$ (Fig. 2d).

Therefore, the decomposition of the CD spectrum may be challenging, but we can still look at the resonance regions where the g-factors ≪1 (Fig. 2d). Fig. 5 (a) shows the spectral derivatives of the COC-CdSe, i.e., $\frac{d\varepsilon}{d\lambda}$. The minima in Fig. 5 (a) are compared with the minima in the CD in Fig. 2b. We look at the minima since they are clearly expressed on the CD spectrum (Fig. 2b). From comparing the wavelengths of the minima of CD and $\frac{d\varepsilon}{d\lambda}$, a remarkable agreement is observed for both (Fig. 5 (b). This confirms our hypothesis that the CD spectrum of COC-NPLs comes from the exciton-LC interaction via the Cotton effect. The LC composites allow a remarkable opportunity to monitor a phase transition with T, as shown in Fig. 6.

We now comment more on the theory of chirality in a hybrid material. Theoretical study by Govorov et al. [36] describes in detail the hybrid material, in which the plasmonic nanocrystal interacts with a discrete optical transition in a chiral bio-medium – the interaction is due to both the near-fields (dipole–dipole) and the far-fields (electromagnetic radiation). However, as it was shown in our earlier paper [37] that the exciton-molecular interaction (dipole–dipole and multipole-dipole) is described by the same formalism since we deal with a noncontact interaction via the electromagnetic fields. Basically, both excitons and plasmons possess dipolar fields that can interact with chiral molecular transitions in neighboring bio-molecular media. For the plasmons, such an interaction is much stronger than for semiconductor QDs and other non-plasmonic nano-materails.[37] But, the NPLs are special! - the

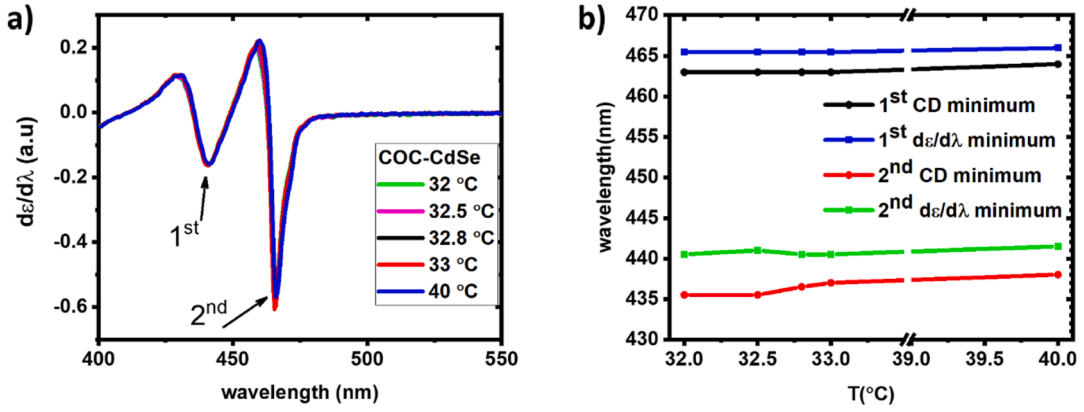

Fig. 5. (a) The derivatives of the absorbance data of COC-CdSe for different temperatures. (b) Plotting the positions of the minima of the absorbance-derivative and CD.

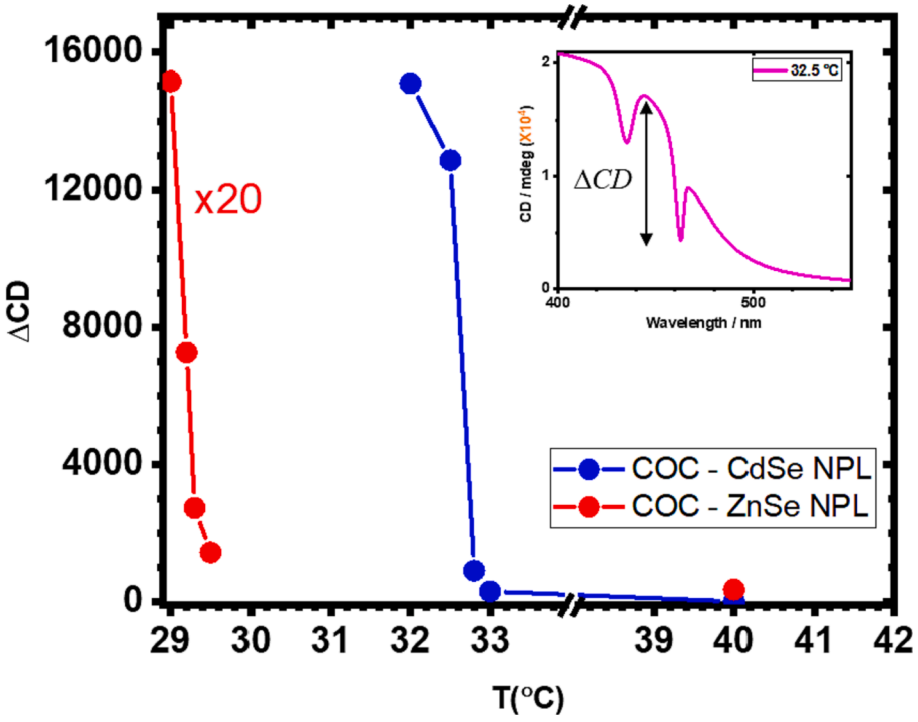

Fig. 6. The NPL-based CD signal as a function of temperature (T) demonstrating the phase transition in the chiral LC matrix.

exciton in the NPL is so strong and sharp that such an interaction becomes strong and prominent in our study here. Finally, we comment that the mechanism of chiral light-matter interaction, which leads to the characteristic CD signals of the type of $CD \propto \frac{d\varepsilon}{d\lambda}$, is universal – it is the so-called Cotton effect [39]. This effect leads to the formation of two separate chiral optical eigen-modes if a material system possesses chiral atomic or nano-scale architecture [36,40]. Origins of the nanocrystal-medium interaction can be diverse, i.e., exciton-molecular coupling (like in here), or plasmon-molecular and optical dielectric interactions. Such a bi-signate behavior is typical for a weak light-matter interaction, whereas, when the interaction becomes strong, the CD line shapes can become much more complex and diverse [41].

3.4. CdSe NPLs in BPLC

To further elucidate the concept of LC-driven NPL assembly, CdSe NPLs were incorporated into left handed (LH) and right handed (RH) blue phase (BP) LC mixtures. The preparation of chiral NPs using BPLC has not been extensively explored in the literature [42]. BPLCs are a class of LCs that exist between the isotropic and cholesteric phases of highly chiral LC mixtures [43]. BPLC mixtures were prepared using a modified protocol reported by Lee et al. [44,45] and the composition can be found in the ESI. The incorporation of NPLs into BPLCs enables the exploration of NPs in both LH and RH LC hosts. More importantly, BPLC-NPL composites form very stable thin films (due to NP stabilization of BP disclination lines) [44] which allows for CD measurements at ambient conditions. The film preparation procedure is described in the ESI. Preliminary dispersion of NPLs (2 and 4 wt% NPL content) in the BPLC mixture showed dominant LC reflection with very weak discernible NPL peaks in the CD spectra as shown in Fig. S15. At these lower concentrations, NPLs disperse in both the disordered disclination lines of BPLCs and the ordered BPLC phase. Subsequent increased loading of 10 wt%, resulted mainly in intercalation of NPLs within the ordered BPLC matrix (due to saturation of the disclination defects [45]). This is corroborated by DSC spectra in Fig. S16 showing significant shifts > 25 °C in the LC phase transition peaks for the 10 % NPL sample but not the 2 % and 4 % NPL samples which exhibited shifts <5 °C. Fig. S17 shows representative films and corresponding absorption spectra for pure BPLC and composites comprised of 2 %, 4 % and 10 % NPLs. The spectra show that the BP feature between 500 and 600 nm is maintained in all samples.

CD spectra for the NPL-BPLC composites (10 % NPL) were collected at four orientations to minimize the effects from linear dichroism, linear birefringence and photoelastic modulator [46]. The spectra (CD and corresponding absorption) for the composites are shown in Fig. 7 a–d.

Averaged CD spectra from the different CD measurements are shown in Fig. 7 (e) and (f) for RH and LH films, respectively. CD spectra of the films follow the handedness of pure BPLC (Fig. S18) as shown by peaks in the negative and positive regions. However, the NPL CD peaks in Fig. 7 (e) and (f) do not show opposite cotton effects in the RH and LH films. These observed chiroptical properties likely stem from the dispersion of NPLs in the ordered LC phase. TEM studies of LH and RH NPL-BPLC composites showed assembled NPLs (Fig. S19). The lack of opposite cotton effects for the NPL CD peaks in LH and RH BPLC-NPLs can be attributed to the fact that NPLs disperse both in the disordered disclination lines and the ordered LC medium.

To better understand this phenomenon, we conducted a series of experiments using a cholesteric liquid crystal (CLC) mixture that is different from the blue phase (BP)-forming mixture. The difference in the two systems lies in the fact that the blue-phase forming LC mixture has disclination lines where nanoparticles tend to accumulate instead of dispersing entirely in the LC medium. The newly prepared LC mixture ensures that nanoparticles disperse entirely in the LC medium. To achieve this, we used a lower concentration (7 %) of chiral dopants (R10 11 and S10 11). The CLC mixture preparation can be found in the ESI. The nanoplatelets (NPL) content in LC was maintained at 10 wt% and 50 μm films were prepared similar to the conditions reported for the BPLC mixture. However, the films were very hazy and non-uniform as shown in Fig. S22. The baseline for the absorption spectra starts at absorbance of 1 and such films were not further characterized. Films with reduced thickness (15 μm) were prepared with the aim of realizing less hazy films for CD measurements. Fig. 8 shows the absorption and CD spectra of 15 μm films prepared with the same NPL-CLC mixture used for the 50 μm films.

The CD spectra showed opposite cotton effects for the NPL exciton

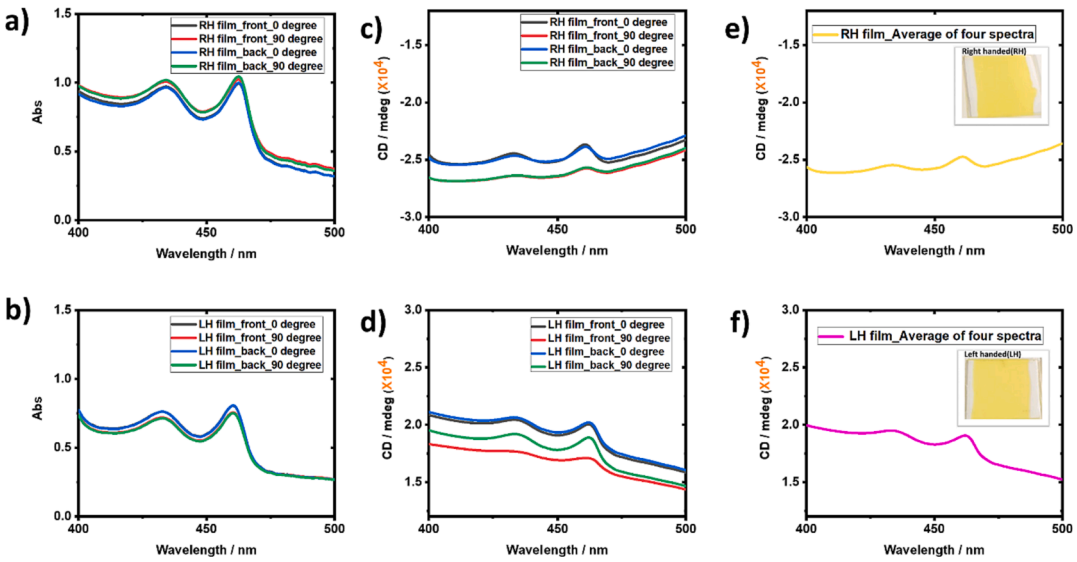

Fig. 7. Absorption spectra of RH (a) and LH (b) BPLC-NPL composites at four orientations. Corresponding CD spectra at four orientations (c and d). Averaged CD spectra (e and f). 50 μm thick films are shown as insets.

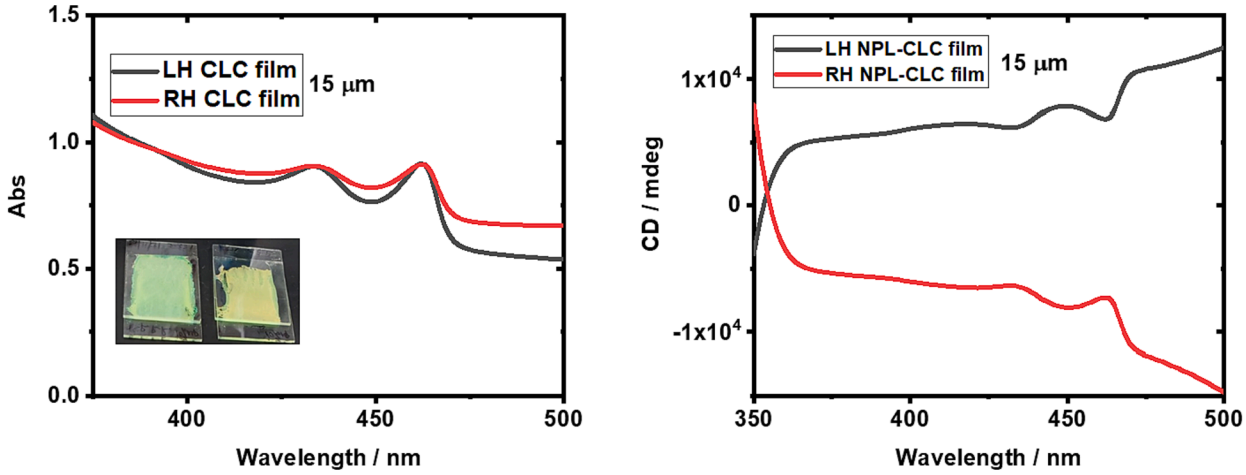

Fig. 8. Absorption (left) and CD spectra (right) of 15 μm CdSe NPL-CLC films.

peaks (432 nm and 462 nm) suggesting LC-induced chirality in CdSe NPLs. As indicated above, the NPLs in the CLC mixture are dispersed entirely in the ordered LC medium unlike the BPLC system where NPLs disperse primarily in the disordered disclination lines and somewhat in the LC medium. We believe this is likely to account for lack of opposite cotton effects in both LH and RH BPLC systems. While the sign of the CD signal is different between the LH and RH BPLC films, the expected peak inversion for the nanoparticles is not observed. The BPLC forms a periodic cubic structure that is seemingly independent of the chirality of the double twisted cylinders. The nanoparticles dispersed in the disclination lines must then be assembled in a separate chiral structure that is similar for both configurations. This phenomenon will be explored in future work.

The figure of merit for the bulk CD signal is the ratio $s = |\Delta CD_{front-back}/CD_{av}|$, derived for the front-back optical configurations; here $\Delta CD_{front-back} = CD_{front,av} - CD_{back,av}$, and CD_{av} is the CD averaged over all 4 configuations [46]. We show in Fig. S20 that $|s|<0.05$ in our case which tells us about high quality of our CD measurements. It shows that our signals come from the 3D bulk chiral property, not from artifacts like non-planar surfaces or tilting a film.

Exploration of ZnSe NPLs in BPLCs at 4 % and 6 % wt. % NPL, resulted in films with 'diminished' NPL peaks as shown by the absorption spectra in Fig. S21. The bigger ZnSe NPLs are more likely to aggregate as observed with COC LC. However, films with lower concentration of ZnSe NPLs, 0.5 % in BPLCs, still did not show distinct NPL peaks (Fig. S21). This observation also strongly suggests that NPLs (both CdSe and ZnSe) interact differently with COC and BPLCs. In the case of ZnSe, the 'degradation' of NPLs is also likely to occur due to the high processing temperature of 200 °C used to prepare the NPL-BPLC composites. Lower temperature approaches for the dispersion of ZnSe NPLs in a variety of BPLC systems are currently ongoing.

4. Conclusion

In summary, LC-driven assembly of CdSe and ZnSe NPLs resulted exciton-induced circular dichroism. We demonstrated reversible and robust circular dichroism properties that are vastly superior to chiral NPLs synthesized with the commonly used chiral thiols. Unlike most literature methods using semiconductor nanoparticles, the approach in this work does not require synthetic surface functionalization of the nanoparticles with mesogenic ligands. This was achieved due to the unique chemical structure of COC liquid crystal which makes the LC

compatible with commonly used nanoparticle ligands. The work also showed that a critical concentration of nanoparticles is needed to minimize dominant LC reflections. More importantly, induced circular dichroism was still realized at temperatures where there was no signal corresponding to the pure LC (COC), suggesting that NPL exciton CD peaks do not come from the LC. LC-induced chirality in NPLs was also demonstrated using a different cholesteric liquid crystal system. Theoretical studies corroborated the concept of LC-induced NPL chirality.

Thin films of CdSe NPL-LC composites were prepared using both RH and LH BPLCs and their chiroptical properties were characterized. However, the NPL CD peaks did not show opposite cotton effects in the RH and LH films and further studies are ongoing to better understand the chiroptical properties of the films. We believe that further improvements in such liquid crystal-nanomaterial composites could benefit potential future applications requiring high polarization discrimination ratios.

CRediT authorship contribution statement

Urice N. Tohgha: Writing – review & editing, Writing – original draft, Visualization, Validation, Methodology, Investigation, Formal analysis, Data curation, Conceptualization. **Kyung Min Lee:** Validation, Data curation, Investigation, Writing – original draft, Writing – review & editing, Visualization. **Joseph M. Slocik:** Visualization, Methodology, Data curation, Conceptualization. **Ecklin M. Crenshaw:** Writing – review & editing, Visualization, Data curation. **Zachary Marsh:** Writing – review & editing, Validation, Investigation. **Oscar A. Ovando:** Investigation, Formal analysis, Data curation. **Alexander O. Govorov:** Writing-review & editing, Visualization, Data curation, Formal analysis. **Nicholas P. Godman:** Writing - review & editing, Writing - original draft, Visulaization, Conceptualization, Supervision.

Declaration of competing interest

The authors declare that they have no known competing financial interests or personal relationships that could have appeared to influence the work reported in this paper.

Data availability

Data will be made available on request.

Acknowledgement

The authors acknowledge funding from the Materials and Manufacturing Directorate of the Air Force Research Laboratory, Wright–Patterson Air Force Base, under contract #FA8650-16–D-5404. A.O.G. acknowledges the ARO grant (contract W911NF-19-20081). A.O. G. thanks the Nanoscale & Quantum Phenomena and Quantitative Biology Institutes (NQPI and QBI) at Ohio University for supporting his research.

Appendix A. Supplementary material

Supplementary data to this article can be found online at https://doi.org/10.1016/j.molliq.2024.124187.

References

[1] M.P. Moloney, Y.K. Gun'ko, J.M. Kelly, Chiral highly luminescent CdS quantum dots, Chem. Commun. 38 (2007) 3900–3902.
[2] Y. Zhou, M. Yang, K. Sun, Z. Tang, N.A. Kotov, Similar topological origin of chiral centers in organic and nanoscale inorganic structures: effect of stabilizer chirality on optical isomerism and growth of CdTe nanocrystals, J. Am. Chem. Soc. 132 (17) (2010) 6006–6013.
[3] U. Tohgha, K.K. Deol, A.G. Porter, S.G. Bartko, J.K. Choi, B.M. Leonard, K. Varga, J. Kubelka, G. Muller, M. Balaz, Ligand induced circular dichroism and circularly polarized luminescence in CdSe quantum dots, ACS Nano 7 (12) (2013) 11094–11102.
[4] A. Ben-Moshe, A. Teitelboim, D. Oron, G. Markovich, Probing the interaction of quantum dots with chiral capping molecules using circular dichroism spectroscopy, Nano Lett. 16 (12) (2016) 7467–7473.
[5] G. Yang, M. Kazes, D. Oron, Chiral 2D colloidal semiconductor quantum wells, Adv. Funct. Mater. 28 (28) (2018) 1802012.
[6] S. Huo, P. Duan, T. Jiao, Q. Peng, M. Liu, Self-assembled luminescent quantum dots to generate full-color and white circularly polarized light, Angew. Chem. Int. Ed. 56 (40) (2017) 12174–12178.
[7] Y. Shi, P. Duan, S. Huo, Y. Li, M. Liu, Endowing perovskite nanocrystals with circularly polarized luminescence, Adv. Mater. 30 (12) (2018) 1705011.
[8] A. Rodarte, C. Ferri, C. Gray, L. Hirst, S. Ghosh, Directed assembly and in situ manipulation of semiconductor quantum dots in liquid crystal matrices, SPIE 8279 (2012).
[9] A.J. Al-Alwani, O.A. Shinkarenko, A.S. Chumakov, M.V. Pozharov, N. N. Begletsova, A.S. Kolesnikova, V.P. Sevostyanova, E.G. Glukhovskoy, Influence of capping ligands on the assembly of quantum dots and their properties, Mater. Sci. Technol. 35 (9) (2019) 1053–1060.
[10] M. Bugakov, N. Boiko, P. Samokhvalov, X. Zhu, M. Möller, V. Shibaev, Liquid crystalline block copolymers as adaptive agents for compatibility between CdSe/ZnS quantum dots and low-molecular-weight liquid crystals, J. Mater. Chem. C 7 (15) (2019) 4326–4331.
[11] Y. Shen, I. Dierking, Perspectives in liquid-crystal-aided nanotechnology and nanoscience, Appl. Sci. 9 (12) (2019) 2512.
[12] C. Blanc, D. Coursault, E. Lacaze, Ordering nano- and microparticles assemblies with liquid crystals, Liq. Cryst. Rev. 1 (2) (2013) 83–109.
[13] L.-J. Chen, J.-D. Lin, C.-R. Lee, An optically stable and tunable quantum dot nanocrystal-embedded cholesteric liquid crystal composite laser, J. Mater. Chem. C 2 (22) (2014) 4388–4394.
[14] A.L. Rodarte, F. Cisneros, J.E. Hein, S. Ghosh, L.S. Hirst, Quantum dot/liquid crystal nanocomposites in photonic devices, Photonics 2 (3) (2015) 855–864.
[15] M.F. Prodanov, N.V. Pogorelova, A.P. Kryshtal, A.S. Klymchenko, Y. Mely, V. P. Semynozhenko, A.I. Krivoshey, Y.A. Reznikov, S.N. Yarmolenko, J.W. Goodby, V.V. Vashchenko, Thermodynamically stable dispersions of quantum dots in a nematic liquid crystal, Langmuir 29 (30) (2013) 9301–9309.
[16] A.L. Rodarte, Z.S. Nuno, B.H. Cao, R.J. Pandolfi, M.T. Quint, S. Ghosh, J.E. Hein, L. S. Hirst, Tuning quantum-dot organization in liquid crystals for robust photonic applications, ChemPhysChem 15 (7) (2014) 1413–1421.
[17] S. Parzyszek, J. Tessarolo, A. Pedrazo-Tardajos, A.M. Ortuño, M. Bagiński, S. Bals, G.H. Clever, W. Lewandowski, Tunable circularly polarized luminescence via chirality induction and energy transfer from organic films to semiconductor nanocrystals, ACS Nano 16 (11) (2022) 18472–18482.
[18] A. Nemati, S. Shadpour, L. Querciagrossa, L. Li, T. Mori, M. Gao, C. Zannoni, T. Hegmann, Chirality amplification by desymmetrization of chiral ligand-capped nanoparticles to nanorods quantified in soft condensed matter, Nat. Commun. 9 (1) (2018) 3908.
[19] S.A. Bhat, D.S.S. Rao, S.K. Prasad, C.V. Yelamaggad, Chiral plasmonic liquid crystal gold nanoparticles: self-assembly into a circular dichroism responsive helical lamellar superstructure, Nanoscale Adv. 3 (8) (2021) 2269–2279.
[20] X. Zhang, Y. Xu, C. Valenzuela, X. Zhang, L. Wang, W. Feng, Q. Li, Liquid crystal-templated chiral nanomaterials: from chiral plasmonics to circularly polarized luminescence, Light Sci. Appl. 11 (1) (2022) 223.
[21] M. Zhang, Y. Wang, Y. Zhou, H. Yuan, Q. Guo, T. Zhuang, Amplifying inorganic chirality using liquid crystals, Nanoscale (2021).
[22] D. Kim, D. Ndaya, R. Bosire, F.K. Masese, W. Li, S.M. Thompson, C.R. Kagan, C. B. Murray, R.M. Kasi, C.O. Osuji, Dynamic magnetic field alignment and polarized emission of semiconductor nanoplatelets in a liquid crystal polymer, Nat. Commun. 13 (1) (2022) 2507.
[23] K. Zuo, H. Shi, X. Yan, J. Liu, Y.-J. Liu, D. Luo, Y. Shi, Full-color and white circularly polarized luminescence from CdSe/ZnS quantum dots by chiral templates of cellulose nanocrystals, J. Mater. Chem. C 10 (39) (2022) 14729–14736.
[24] X. Gao, X. Zhang, L. Zhao, P. Huang, B. Han, J. Lv, X. Qiu, S.-H. Wei, Z. Tang, Distinct excitonic circular dichroism between wurtzite and zincblende CdSe nanoplatelets, Nano Lett. 18 (11) (2018) 6665–6671.
[25] Y. Pang, M. Zhang, D. Chen, W. Chen, F. Wang, S.J. Anwar, M. Saunders, M. R. Rowles, L. Liu, S. Liu, A. Sitt, C. Li, G. Jia, Why do colloidal wurtzite semiconductor nanoplatelets have an atomically uniform thickness of eight monolayers? J. Phys. Chem. Lett. 10 (12) (2019) 3465–3471.
[26] D.A. Kurtina, V.P. Grafova, I.S. Vasil'eva, S.V. Maksimov, V.B. Zaytsev, R. B. Vasiliev, Induction of chirality in atomically thin ZnSe and CdSe nanoplatelets: strengthening of circular dichroism via different coordination of cysteine-based ligands on an ultimate thin semiconductor core, Materials 16 (3) (2023) 1073.
[27] B.T. Diroll, B. Guzelturk, H. Po, C. Dabard, N. Fu, L. Makke, E. Lhuillier, S. Ithurria, 2D II–VI semiconductor nanoplatelets: from material synthesis to optoelectronic integration, Chem. Rev. 123 (7) (2023) 3543–3624.
[28] L. Hirst, J. Kirchhoff, R. Inman, S. Ghosh, Quantum dot self-assembly in liquid crystal media, SPIE 7618 (2010).
[29] L. Guillemeney, L. Lermusiaux, G. Landaburu, B. Wagnon, B. Abécassis, Curvature and self-assembly of semi-conducting nanoplatelets, Commun. Chem. 5 (1) (2022) 7.
[30] J. Yeom, U.S. Santos, M. Chekini, M. Cha, A.F. de Moura, N.A. Kotov, Chiromagnetic nanoparticles and gels, Science 359 (6373) (2018) 309.
[31] X. Gao, B. Han, X. Yang, Z. Tang, Perspective of chiral colloidal semiconductor nanocrystals: opportunity and challenge, J. Am. Chem. Soc. 141 (35) (2019) 13700–13707.

[32] J.J. Ou, S.H. Chen, Simulation of circular dichroism by chromophores coupled with selective reflection by cholesteric stacks, J. Phys. Chem. B 124 (4) (2020) 679–683.
[33] E. Sackmann, J. Voss, Circular dichroism of helically arranged molecules in cholesteric phases, Chem. Phys. Lett. 14 (4) (1972) 528–532.
[34] H.S. Oh, G.S. He, W.-C. Law, A. Baev, H. Jee, X. Liu, A. Urbas, C.-W. Lee, B.L. Choi, M.T. Swihart, P.N. Prasad, Manipulating nanoscale interactions in a polymer nanocomposite for chiral control of linear and nonlinear optical functions, Adv. Mater. 26 (10) (2014) 1607–1611.
[35] Cao, Q.; Song, R.; Chan, C. C. S.; Wang, Z.; Wong, P. Y.; Wong, K. S.; Blum, V.; Lu, H., Chiral perovskite nanoplatelets with tunable circularly polarized luminescence in the strong confinement regime, Adv. Opt. Mater. n/a (n/a), 2203125.
[36] A.O. Govorov, Z. Fan, Theory of chiral plasmonic nanostructures comprising metal nanocrystals and chiral molecular media, ChemPhysChem 13 (10) (2012) 2551–2560.
[37] A.O. Govorov, Z. Fan, P. Hernandez, J.M. Slocik, R.R. Naik, Theory of circular dichroism of nanomaterials comprising chiral molecules and nanocrystals: plasmon enhancement, dipole interactions, and dielectric effects, Nano Lett. 10 (4) (2010) 1374–1382.
[38] A.O. Govorov, Plasmon-Induced Circular Dichroism of a Chiral Molecule in the Vicinity of Metal Nanocrystals. Application to Various Geometries, J. Phys. Chem. C 115 (16) (2011) 7914–7923.
[39] G.D. Fasman, Circular dichroism and the conformational analysis of biomolecules, 1996.
[40] O. Ávalos-Ovando, E.Y. Santiago, A. Movsesyan, X.-T. Kong, P. Yu, L.V. Besteiro, L. K. Khorashad, H. Okamoto, J.M. Slocik, M.A. Correa-Duarte, M. Comesaña-Hermo, T. Liedl, Z. Wang, G. Markovich, S. Burger, A.O. Govorov, Chiral bioinspired plasmonics: a paradigm shift for optical activity and photochemistry, ACS Photonics 9 (7) (2022) 2219–2236.
[41] A. Movsesyan, L.V. Besteiro, X.-T. Kong, Z. Wang, A.O. Govorov, Engineering strongly chiral plasmonic lattices with achiral unit cells for sensing and photodetection, Adv. Opt. Mater. 10 (14) (2022) 2101943.
[42] M. Zhang, Y. Wang, Y. Zhou, H. Yuan, Q. Guo, T. Zhuang, Amplifying inorganic chirality using liquid crystals, Nanoscale 14 (3) (2022) 592–601.
[43] G. Cordoyiannis, M. Lavrič, V. Tzitzios, M. Trček, I. Lelidis, G. Nounesis, S. Kralj, J. Thoen, Z. Kutnjak, Experimental advances in nanoparticle-driven stabilization of liquid-crystalline blue phases and twist-grain boundary phases, Nanomaterials 11 (11) (2021) 2968.
[44] K.M. Lee, U. Tohgha, T.J. Bunning, M.E. McConney, N.P. Godman, Effect of amorphous crosslinker on phase behavior and electro-optic response of polymer-stabilized blue phase liquid crystals, Nanomaterials 12 (1) (2022) 48.
[45] U.N. Tohgha, E.P. Crenshaw, M.E. McConney, K.M. Lee, N.P. Godman, Tuning of optical properties and phase behavior of Nanomaterial-stabilized blue phase liquid crystals, J. Colloid Interface Sci. 639 (2023) 401–407.
[46] Y. Yao, T.J. Ugras, T. Meyer, M. Dykes, D. Wang, A. Arbe, S. Bals, B. Kahr, R. D. Robinson, Extracting pure circular dichroism from hierarchically structured CdS magic cluster films, ACS Nano 16 (12) (2022) 20457–20469.